Hue University Journal of Science: Natural Science
Vol. 132, No. 1B, 113–121, 2023

pISSN 1859-1388
eISSN 2615-9678

# Modification of Phu Yen diatomite and its application to Cr(VI) removal in aqueous medium

**Tran Vinh Thien***

Faculty of Environment, Ho Chi Minh City University of Natural Resources and Environment, Vietnam

* Correspondence to Tran Vinh Thien <tvthien@hcmunre.edu.vn>

(*Received: 23 September 2022; Accepted: 30 March 2023*)

**Abstract.** In this study, we successfully prepared a carboxyl-rich carbon nanomaterial from Phu Yen natural diatomite and used it as an effective adsorbent to remove Cr(VI) in aqueous media. The obtained nanomaterial was characterized by means of XRD, SEM, EDS, and FT-IR. The adsorption characteristics of Cr(VI) were investigated. pH has a significant influence on the adsorption process, and pH = 1 is optimal for Cr(VI) adsorption at ambient temperature. Three types of materials were prepared, including natural diatomite (DE), modified diatomite with carbon nanomaterial (DE/S), and modified diatomite with carboxyl-rich carbon nanomaterial (DE/C-S), and DE/C-S exhibits the highest adsorption capacity under the optimal conditions. The pseudo-second-order kinetic model and the Langmuir isotherm well describe the adsorption process of Cr(VI) onto DE/C-S with the maximum adsorption capacity of 58.82 $mg \cdot g^{-1}$, which is significantly higher compared with that of the natural diatomite (2.29 $mg \cdot g^{-1}$). Carboxyl-rich carbon-modified diatomite nanomaterials have great potential for use in removing Cr(VI) from wastewater.

**Keywords:** diatomite, modification, adsorption, Cr(VI)

## 1 Introduction

Water pollution, especially heavy-metal pollution, has had a negative impact on human life and health. Hexavalent chromium or Cr(VI) is a form of metallic elemental chromium and is generally generated in industrial processes. Being used in the manufacture of stainless steel, textiles, anticorrosion coatings, and leather tanning, Cr(VI) gets into drinking water through industrial pollution. It is also present naturally in some minerals. The US Environmental Protection Agency sets the maximum contaminant level (MCL) for total chromium at 100 $\mu g \cdot L^{-1}$ in drinking water [1]. Meanwhile, Vietnam's National Technical Regulation on Domestic Water Quality (QCVN 01-1:2018/BYT) sets MCL for total chromium at 50 $\mu g \cdot L^{-1}$ [2]. The total chromium MCL is established to address exposures to Cr(VI), a more toxic form of chromium [1].

Various technologies were developed to remove Cr(VI) worldwide, such as adsorption, chemical precipitation, photocatalytic reduction, membrane separation, electrodeposition, and ion exchange. Among them, adsorption is advantageous regarding easy operation, lower operating costs, and fewer secondary products [3].

In Vietnam, Phu Yen province has a significant reserve of diatomaceous earth (estimated at 69 million $m^3$) with high quality ($SiO_2$ content over 50%). Diatomite is composed mainly of silicon oxide $SiO_2$ and some other oxides. The diatomaceous earth structure consisting of microcapillary systems interspersed with macrocapillaries is an ideal adsorbent or

catalyst carrier. Numerous studies have shown that diatomite's modification by attaching surface-active sites can form selective and effective adsorbents [4, 5].

This paper presents the surface modification of Phu Yen diatomite with carboxyl-rich carbon nanomaterials and determines its adsorption capacity for Cr(VI).

## 2 Material and methods

### 2.1 Material

Raw diatomite was obtained from Hoa Loc in Tuy An district, Phu Yen province, Vietnam. It was then calcined at 700 °C, finely crushed and sifted. After the organic impurities were removed, the product was dried at 100 °C and stored in a glass bottle with a ground stopper in an oven at 60 °C.

Deionized water was used throughout the whole experiment. Sucrose ($C_{12}H_{22}O_{11}$), acrylic acid ($C_3H_4O_2$), potassium dichromate ($K_2Cr_2O_7$), hydrochloric acid (HCl), sodium hydroxide (NaOH), and other chemicals used in the experiments are of analytical grade.

### 2.2 Preparation of carbon-modified diatomite nanomaterial

The diatomite-carbon nanocomposite (denoted as DE/S) was prepared from sucrose, as a carbon source, and a carrier. Disperse 4 g of diatomite in 110 mL of sucrose solution (containing 12 g of sucrose). Similarly, a carboxyl-rich carbon-diatomite nanocomposite (denoted as DE/C-S) was prepared by dispersing 4 g of diatomite in 110 mL of a mixed solution of sucrose and acrylic acid (containing 12 g of sucrose and 16 mL acrylic acid). The solutions were exposed to ultrasound for 15 min at ambient temperature to form a stable suspension and placed in a stainless steel-coated Teflon autoclave. The autoclave was placed in an oven at 180 °C for 24 h. The obtained products were cooled to ambient temperature, centrifuged at 1,000 rpm for 8 min, washed with double distilled water, and dried at 60 °C for 24 h.

### 2.3 Material characterisation

The natural and modified diatomite materials were characterised by using X-ray diffractoscopy (XRD), scanning electron microscopy (SEM), X-ray energy-dispersive diffractometry (EDS), and infrared spectroscopy (FT-IR).

X-ray diffractograms of the samples were recorded on a Bruker AXS/D8 ADVANCE ECO diffractometer, giving information on the material phase composition and crystal structure. Scanning electron microscopic images, recorded on a JSM-5300 microscope, were used to study the surface morphology of the materials. X-ray energy-dispersive diffractograms, recorded on a JEOL JED 2300, provided information on the elemental composition of the material's surface. Infrared (FT-IR) spectra were recorded with a Nicolet IS5 spectrometer at the wave number of 400–4000 $cm^{-1}$ at ambient temperature with solid KBr. FT-IR was used to determine the specific functional groups on the material surface.

The point of zero charge ($pH_{PZC}$) of the material was determined by placing 0.5 g of the material in conical flasks containing a 0.1 M NaCl solution with a $pH_i$ (initial pH) from 2 to 12 (adjusted with 0.1 M NaOH or 0.1 M HCl solutions). The mixtures were stirred for 48 h, and the final pH value of the solution was recorded ($pH_f$). The intersection of the curve representing the relationship between $\Delta pH$ ($pH_f - pH_{i)}$ and $pH_i$ with the horizontal axis gives the $pH_{PZC}$ of the material.

### 2.4 Batch adsorption experiments

In this study, the Cr(VI) adsorption onto the adsorbent was conducted in batches at ambient

pISSN 1859-1388
eISSN 2615-9678

temperature. First, place 0.1 g of DE, DE/S, or DE/C-S in a conical flask containing 50 mL of a potassium dichromate ($K_2Cr_2O_7$) solution with a known concentration at a defined pH. Then, stir the mixture continuously with a magnetic stirrer. After a certain time, the mixture was filtered to separate the solids, and the concentration of Cr(VI) in the obtained solution was determined by using an Evolution 350 UV-Vis spectrophotometer at 540 nm [6]. The adsorption capacity of the adsorbents at time $t$ under the investigation conditions was calculated according to formula (1).

$$q_t = \frac{(C_0 - C_t) \times V}{m} \quad (1)$$

where $C_0$ and $C_t$ are the initial metal ion concentrations and at time $t$ (mg·L$^{-1}$); $V$ is the volume of metal ion solution (L); $m$ is the mass of the adsorbent (g).

The content of metal ions in the solution adsorbed at time $t$, also known as the adsorption efficiency $H$, was calculated according to formula (2).

$$H\% = \frac{C_0 - C_t}{C_0} \times 100 \quad (2)$$

In the following part, the adsorption equilibrium time for the materials was determined by monitoring the metal ion concentration during the adsorption process until this value remained stable with time. The metal ion concentration and the adsorption capacity at equilibrium are denoted as $C_e$ and $q_e$. The studies on adsorption equilibrium with different initial concentrations of Cr(VI) ion were conducted to describe the adsorption capacity of the materials.

The dependence of adsorption capacity of the materials on pH from 1 to 7 (the pH was adjusted with 0.1 M NaOH or 0.1 M HCl solutions) was studied. The pH value for the maximum adsorption capacity was set for further investigation experiments.

## 3 Results and discussion

### 3.1 Characterization of materials

**SEM and EDS analysis**

The SEM images of DE, DE/S, and DE/C-S samples are presented in Fig.s 1a, 1b, and 1c. It is evident that Phu Yen diatomite is formed from 10 μm long tubes with a diameter of several micrometres (Fig. 1a). On the wall of the tube, there are capillaries with diameters ranging from a few tens to several hundred nanometers. These capillaries render diatomite a highly effective adsorbent. The materials modified with sucrose alone and with sucrose and acrylic acid have the same structure as DE. However, their surface becomes rougher because it is covered by a layer of spherical particles with the size of several tens of nanometres. The coverage is in the following order: DE/C-S > DE/S > DE. It is possible that this increased surface area is relative to DE in the order above.

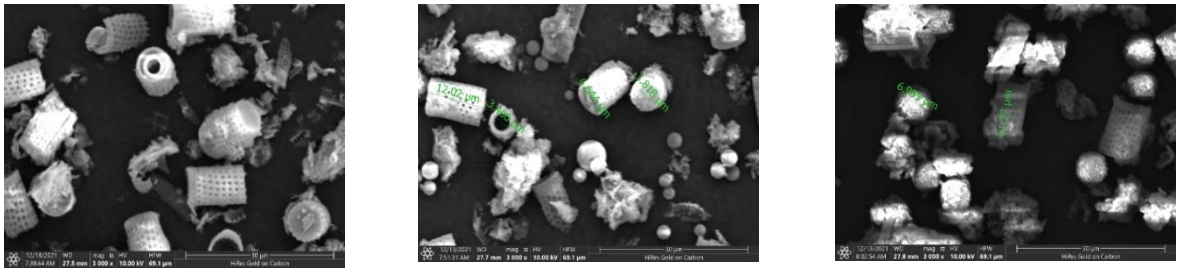

(a) (b) (c)

**Fig. 1.** SEM images of DE (a), DE/S (b), and DE/C-S (c) samples

The EDS spectra and the average elemental composition of the respective material samples are given in Table 1 and Fig. 2.

It is obvious that the mass percentage of carbon in the modified samples is much higher than that of natural diatomite, while the mass composition of oxygen, silicon, aluminum, and iron significantly decreases. Thus, the modification of diatomite augments the carbon content and may increase the ratio of C=O and COO-functional groups and, at the same time, reduces the number of Si-containing functional groups, such as Si–O and Si–OH in the material.

**Table 1.** Elemental composition of DE, DE/S, and DE/C-S samples

| Element | Mass composition, % | | |
|---|---|---|---|
| | DE | DE/S | DE/C-S |
| C | 8.96 | 48.56 | 40.13 |
| O | 57.73 | 43.47 | 45.34 |
| Si | 27.52 | 6.66 | 12.47 |
| Al | 3.93 | 1.03 | 1.48 |
| Fe | 1.86 | 0.28 | 0.86 |

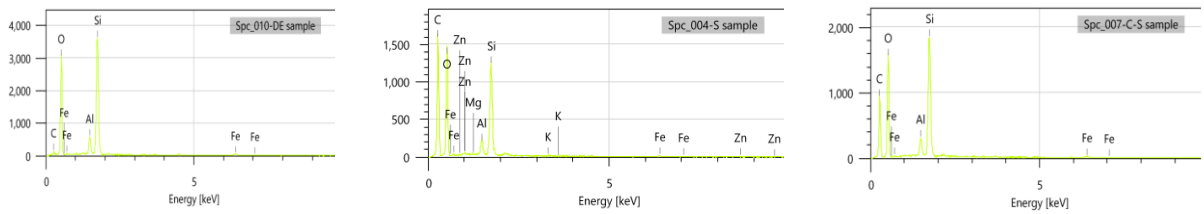


(a) (b) (c)

**Fig. 2.** EDS of DE (a), DE/S (b), and DE/C-S (c) samples

**XRD**

The XRD patterns of DE, DE/S, and DE/C-S samples are presented in Fig. 3. The results show that Phu Yen diatomite exists mainly in the amorphous form [7]. This observation is also consistent with studies of other diatomite materials worldwide. The XRD patterns of the modified materials also show relatively obtuse peaks, similar to DE, indicating that all three materials are mainly in the amorphous form. Therefore, no change in the crystal structure of Phu Yen diatomite occurs upon modification.

**Infrared spectroscopy**

The infrared spectra of the materials are shown in Fig. 4. The DE's absorption peaks at 1043 and 799 $cm^{-1}$ can be assigned to the stretching vibration of the Si–O–Si group and the bending vibration of the Si–OH group. The absorption band at about 3412 $cm^{-1}$ is attributed to the stretching vibration of the OH group in the water molecules adsorbed onto the material [4].

Thus, diatomite contains Si–O–Si and Si–OH groups on the surface to facilitate adsorption. Meanwhile, the spectra of DE/S and DE/C-S, in addition to these absorption peaks, contain peaks at 2932 and 2950 $cm^{-1}$, attributed to the valence vibration of the C–H bond, 1718 and 1490 $cm^{-1}$ to the stretching vibration of the C=O carboxyl group, and 1640 $cm^{-1}$ to the C=C bond [3]. In addition, the peaks at 1043 and 799 $cm^{-1}$ in the spectra, assigned to the vibrations of the Si–O–Si and Si–OH groups of diatomite, have a significantly decreased intensity. Characteristic peaks for the vibrations of the C–H, C=O, and C=C bonds are also present. These results show

pISSN 1859-1388
eISSN 2615-9678

that the modification creates a composite material between carbon nanoparticles and diatomite. These results are also consistent with those obtained from SEM and EDS studies, allowing us to expect a higher adsorption capacity of the modified materials compared with natural diatomite.

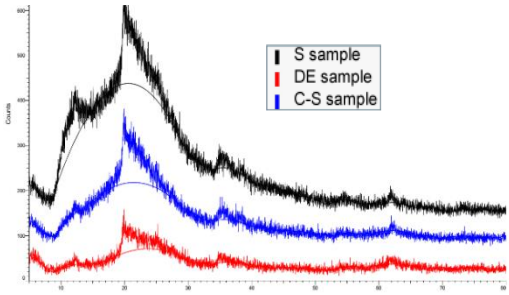


**Fig. 3.** Small angle XRD of DE, DE/S, and DE/C-S samples

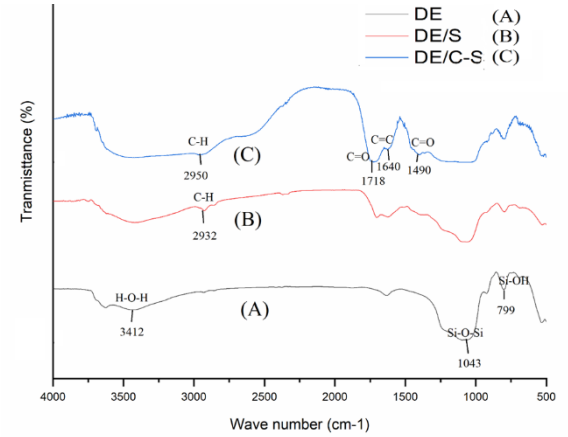


**Fig. 4.** FT-IR of DE (A), S (B), and C-S (C) samples

### 3.2 Adsorption studies

#### Effect of time

Fig. 5 shows that the adsorption capacity of DE is relatively low under experimental conditions (pH 1 and an initial concentration of 84.71 mg·L$^{-1}$). This low $q_t$ is explained by the fact that the surface of DE is negatively charged, which repulses the $CrO_4^{2-}$ and $Cr_2O_7^{2-}$ ions formed in the reaction. Meanwhile, both modified materials, DE/S and DE/C-S, have a higher adsorption capacity. The DE/C-S material has the highest Cr(VI) adsorption capacity, demonstrating that the modification of the diatomite surface with acrylic acid increased the adsorption and removal of Cr(VI) in the solution. The results in Fig. 5 also show that the time for the adsorption to reach equilibrium for DE, DE/S, and DE/C-S materials is about 4, 7, and 9 h, respectively.

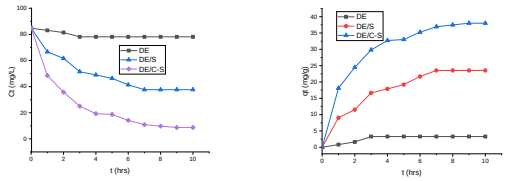


(A) (B)

**Fig. 5.** Time dependence of concentration (A) and adsorption capacity (B) of DE, DE/S, DE/C-S materials in Cr(VI) removal (Experimental conditions: pH 1, initial concentration 84.71 mg·L$^{-1}$)

#### Effect of pH

The effect of pH on the adsorption capacity of DE/C-S was studied at the initial solution concentration of 160 mg·L$^{-1}$, and in this case, the adsorption reached equilibrium after 9 h. The results presented in Fig. 6A show that at pH 1, the adsorption capacity of DE/C-S for Cr(VI) has the maximum value.

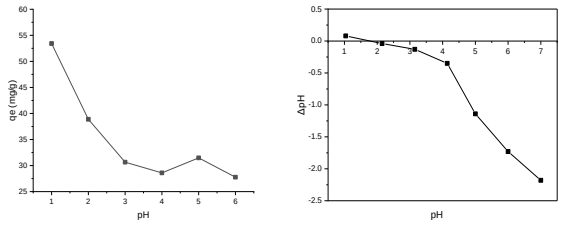


(A) (B)

**Fig. 6.** Change in adsorption capacity with solution pH (A) and point zero charge of DE/C-S surface (B)

It is evident that the adsorption capacity of DE/C-S decreased with pH (Fig. 6A). At pH 1, lower than $pH_{PZC}$ (1.6), the surface of the material is positively charged, while Cr(VI) in solution mainly exists in the $HCrO_4^-$ form, resulting in enhanced adsorption due to electrostatic attraction. When the solution pH is higher than $pH_{PZC}$, the surface becomes negatively charged,

while $HCrO_4^-$ gradually converts to $CrO_4^{2-}$, inhibiting the Cr(VI) uptake on DE/C-S. Therefore, the removal efficiency gradually decreased as pH increased. This change is also consistent with the information on the point of zero charge of DE/C-S materials, which is 1.6, as shown in Fig. 6B. pH 1 was chosen for further studies.

**Adsorption kinetics**

The study of adsorption kinetics allows us to choose a suitable kinetic model. This model describes the adsorption process and suggests the mechanism and rate-controlling stages. In addition, adsorption kinetics provides essential information for applying adsorption processes to wastewater treatment because adsorption kinetic models can be used to predict pollutant removal rates from aqueous solutions in the design of wastewater treatment projects [8]. In this study, we used the two most common models to describe the adsorption process: the pseudo-first-order and the pseudo-second-order kinetic models.

The pseudo-first-order kinetic equation describes the factors affecting the adsorption capacity of the solid phase, usually expressed as formula (3) [8],

$$\frac{dq_t}{dt} = k_1 \times (q_e - q_t)$$

and the linear form is

$$\ln(q_e - q_t) = \ln q_e - k_1 \times t \quad (3)$$

If the adsorption process follows the pseudo-first-order kinetic law, the plot of $\ln(q_e - q_t)$ versus $t$ should give a linear relationship where $k_1$ and $q_e$ can be determined from the slope and intercept of the plot.

The pseudo-second-order adsorption kinetics equation also represents the factors affecting the adsorption capacity of the solid phase. This model is consistent with the hypothesis that chemisorption is a rate-controlling step, expressed as formula (4) [8],

$$\frac{dq}{dt} = k_2 \times (q_e - q_t)^2$$

and the linear form is

$$\frac{t}{q_t} = \frac{1}{k_2 \times q_e^2} + \frac{t}{q_e} \quad (4)$$

If the Cr(VI) adsorption onto material fits the pseudo-second-order kinetics model, the plot of $t/q_t$ versus $t$ should give a linear relationship, and values $k_2$ and $q_e$ can be determined from the slope and intercept of the line.

**Table 2.** Kinetic parameters and predicted correlation coefficients calculated from pseudo-first-order and pseudo-second-order models representing Cr(VI) adsorption of Cr(VI) onto DE, DE/S, and DE/C-S materials

| Materials | Pseudo-first-order | | | Pseudo-second-order | | |
|---|---|---|---|---|---|---|
| | $k_1$ | $q_{e,cal}$ | $R^2$ | $k_2$ | $q_{e,cal}$ | $R^2$ |
| DE | 0.683 | 2.83 | 0.874 | 0.287 | 3.48 | 0.9958 |
| DE/S | 0.448 | 23.21 | 0.952 | 0.032 | 30.96 | 0.9957 |
| DE/C-S | 0.386 | 33.98 | 0.964 | 0.023 | 34.05 | 0.9988 |

Table 2 presents the calculated values of kinetic parameters and the predicted correlation coefficients for the two models. The adsorption according to the pseudo-second-order model for different concentrations is shown in Fig. 7. It is obvious that the pseudo-second-order model gives higher correlation coefficients ($R^2 > 0.99$) than the pseudo-first-order kinetic model for all data. The values of $q_e$ calculated from the second-order model are close to the $q_e$ obtained from experiments. Therefore, the pseudo-second-order model is suitable to describe the adsorption of Cr(VI) ions onto Phu Yen diatomite and its modified materials.

pISSN 1859-1388
eISSN 2615-9678

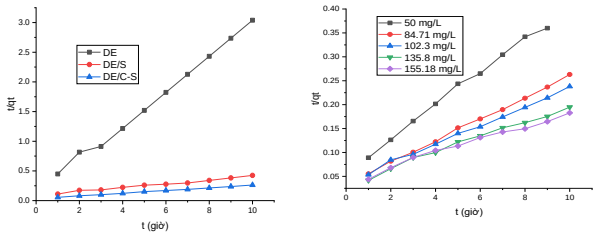


(a) (b)

**Fig. 7.** Adsorption of Cr(VI) ion onto a) DE, DE/S, and DE/C-S materials at the same initial concentration of Cr(VI) 84.71 mg·L$^{-1}$; b) DE/C-S materials at different concentrations, according to pseudo-second-order model

## Adsorption isotherm study

The objective of the adsorption isotherm study is to obtain information on the adsorption process, such as maximum adsorption capacity and the most appropriate correlations for equilibrium curves, and optimize the design of an adsorption system. In this study, two most popular isotherm models were used to describe the adsorption equilibrium with a linear form: Langmuir (formula (5)) and Freundlich (formula (6)) [8].

$$\frac{C_e}{q_e} = \frac{C_e}{q_m} + \frac{1}{K_L \times q_m} \quad (5)$$

$$\ln q_e = \ln K_F + \frac{1}{n} \times \ln C_e \quad (6)$$

where $q_e$ (mg·g$^{-1}$) is adsorption capacity at equilibrium; $q_m$ (mg·g$^{-1}$) is the maximum adsorption capacity corresponding to state where all sites on the adsorbent surface are occupied; $K_L$ is the Langmuir adsorption constant (L·mg$^{-1}$); $C_e$ is the concentration of Cr(VI) ions in the liquid phase at the time of equilibrium (mg·L$^{-1}$) [9, 10]; $K_F$ ((mol·kg$^{-1}$)/(mol·L$^{-1}$)$^n$) is the Freundlich constant, and $1/n$ is the coefficient characterising the heterogeneity of the adsorbent surface.

The data obtained from the adsorption experiments at different concentrations were used to consider the fit of the Langmuir and Freundlich models. The results are shown in Fig. 8, and the parameters of the models are presented in Table 3. The parameters indicate that the adsorption of Cr(VI) ions onto all three materials follows the Langmuir model. This result shows that the adsorption process mainly occurs in monolayers and is ionic in nature.

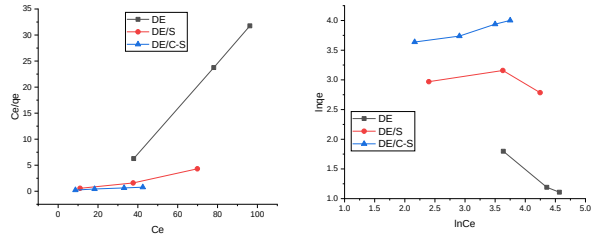


(a) (b)

**Fig. 8.** Langmuir (a) and Freunlich isotherm models (b) for the adsorption of Cr(VI) onto DE, DE/S, and DE/C-S materials at ambient temperature

**Table 3.** Parameters of isotherm models of Cr(VI) adsorption onto DE, DE/S, and DE/C-S materials

| Material | Langmuir model | | | Freundlich model | | |
|---|---|---|---|---|---|---|
| | $K_L$ (L·mg$^{-1}$) | $q_m$ (mg·g$^{-1}$) | $R^2$ | $K_F$ ((mol·kg$^{-1}$)/(mol·L$^{-1}$)$^n$) | $1/n$ | $R^2$ |
| DE | –0.423 | 2.29 | 0.996 | 6.211 | 0.152 | 0.99 |
| DE/S | 0,14 | 14.77 | 0,986 | 24.337 | –0.064 | 0.105 |
| DE/C-S | 0.195 | 58.82 | 0.998 | 22.23 | 0.236 | 0.96 |

From the Langmuir equation, it is possible to calculate the maximum adsorption capacity of the nanocomposite materials obtained via the modification of Phu Yen diatomite for the Cr(VI) ion. The material modified with acrylic acid has a much higher $q_m$ than that of the material modified with carboxyl-rich materials and natural diatomite (58.82, 14.77, and 2.29 mg·g$^{-1}$, respectively). They are compared with other materials in Table 4. Hence, by modifying natural diatomite, we created a new material capable of adsorption and removal of Cr(VI) ions with a high efficiency.

**Table 4.** Maximum Cr(VI) adsorption capacity of different materials

| No. | Material | Condition | $q_m$ (mg·g$^{-1}$) | References |
|---|---|---|---|---|
| 1 | Red mud (activated by $H_2SO_4$) | stirring 80 $^oC$/1 h | 2.34 | Vu Xuan Minh et al. [11] |
| 2 | Coconut sawdust (activated by $H_2SO_4$) | 80 $^oC$/12 h | 3.46 | Selvi et al. [12] |
| 3 | Carbon nanotubes (CNTs) | – | 9.5 | Di et al. [13] |
| 4 | Activated carbon prepared from peanut shells | – | 16.26 | Al-Qthman et al. [14] |
| 5 | Tea grounds (activated by KOH) | – | 52.083 | Do Tra Huong et al. [15] |
| 6 | Rice husk (activated by HCHO) | 30 $^oC$/ 5 h | 59.52 | Le Thi Tinh [16] |
| 7 | Modified diatomite rich in nano carboxyl carbon | Stirring 30 ± 2 $^oC$/8 h | 58.82 | This study |

## 4 Conclusion

The modification of the Phu Yen diatomite surface with carboxyl-rich materials created a nanocarbon composite material with an unchanged surface structure, covered with carbon nanoparticles rich in carboxyl groups and high adsorption capacity for the Cr(VI) removal from aqueous media. The adsorption of Cr(VI) onto the material had an optimal efficiency at pH 1 and followed the pseudo-second-order kinetic model with the adsorption rate increasing in the order of DE, DE/S, and DE/C-S. With the DE/S and DE/C-S materials, the adsorption reached equilibrium after nine hours of stirring. The adsorption of Cr(VI) onto the materials at ambient temperature followed the Langmuir isotherm model, with a maximal adsorption capacity of 58.82 mg·g$^{-1}$. This value is much higher than that of materials modified with carbon, natural diatomite, and other materials. Hence, carboxyl-rich modified diatomite nanomaterial could remove Cr(VI) from wastewater.

## References


1. USEPA. Chromium in Drinking Water. EPA; 2022.
2. QCVN 01-1:2018/BYT. Hanoi: National technical regulation on Domestic Water Quality; 2018.
3. Chen L-F, Liang H-W, Lu Y, Cui C-H, Yu S-H. Synthesis of an Attapulgite Clay@Carbon Nanocomposite Adsorbent by a Hydrothermal Carbonization Process and Their Application in the Removal of Toxic Metal Ions from Water. Langmuir. 2011;27(14):8998-9004.
4. Hossam EGMMB. Diatomite: Its Characterization, Modifications and Applications, Asian Journal of Materials Science 2010;2(3):121-136.
5. Khieu DQ, Hoa TT, Thien TV. Study on adsorption process of methylene blue by Phu Yen diatomte: kinetics, thermodynamics and adsorption isotherms. Journal of Chemistry. 2010;48(2):163-168. (in Vietnamese)
6. ISO 11083:1994. Water quality - Determination of chromium(Vl) - Spectrometric method using 1,5-diphenylcarbazide; 2021.
7. Thien TV, Tu NTT, Son BHD. Study on the modification of Phu Yen diatomite by mixed Fe-Mn oxide and the use of the modified material as an arsenic removal adsorbent in water environment. Vietnam Journal of Catalysis and Adsorption. 2020;10(1):13-20. (in Vietnamese)
8. Ola A. Kinetic and isotherm studies of copper (II) removal from wastewater using various adsorbents. Egytian Journal of Aquatic Research. 2007;33(1):125-143.

pISSN 1859-1388
eISSN 2615-9678

9. Ho YS, McKay G, Was, DAJ, Foster CF. Study of the sorption of divalent metal ions on to peat. Adsorption Science & Technology. 2000;18:639-650.

10. Yuan P, Liu D, Fan M, Yang D, Zhu R, Ge F, et al. Removal of hexavalent chromium [Cr(VI)] from aqueous solutions by the diatomite-supported/unsupported magnetite nanoparticles. Journal of Hazardous Materials. 2010;173(1):614-21.

11. Minh VX, Dung NT, My NT, Huong LTM. Study on the activation of red mud by sulfuric acid and investigate the adsorption capacity of Cr(VI). Vietnam Journal of Chemistry. 2015;53(4):475-479. (in Vietnamese)

12. Selvi K, Pattabhi S, Kadirvelu K. Removal of Cr(VI) from aqueous solution by adsorption onto activated carbon. Bioresource Technology. 2001;80(1):87-9.

13. Di Z-C, Ding J, Peng X-J, Li Y-H, Luan Z-K, Liang J. Chromium adsorption by aligned carbon nanotubes supported ceria nanoparticles. Chemosphere. 2006;62(5):861-5.

14. Al-Othman ZA, Ali R, Naushad M. Hexavalent chromium removal from aqueous medium by activated carbon prepared from peanut shell: Adsorption kinetics, equilibrium and thermodynamic studies. Chemical Engineering Journal. 2012;184:238-47.

15. Huong DT, Thanh DV, Khue MQ, Ngan NTK. Adsorption of Cr(VI) in aqueous medium by KOH modified tea residue adsorbent. Vietnam Journal of Chemistry. 2016;54(1). (in Vietnamese)

16. Tinh LT. Study on Cr adsorption capacity on rice husks and treatment applications to separate Cr from wastewater [Master thesis]. Hanoi: Hanoi University of Natural Science; 2011. (in Vietnamese)